

Geometrically Optimized, LaBr₃:Ce Scintillation Sensor Array for Enhanced Stand-Off Direction Finding of Gamma Radiation Sources

James H. Winso *Member, IEEE*, Eric S. Ackermann, Michael Fennell, Roger Perez, John Rolando, Manish Pagey, Raulf Polichar, Juan Martinez, Jens Hovgaard, Greg Kogut, H. R. (Bart) Everett, Donnie Fellars, Joel Baumbaugh, Gary Mastny

Abstract—A Radiation Source Identification and Targeting (RadSITE™) innovation has been conceptually demonstrated that remotely detects and identifies one or more Localized Gamma Sources simultaneously and also provides Azimuth Directions of each source. The innovation exploits the superior energy resolution of Cerium Doped Lanthanum Bromide (LaBr₃:Ce) Scintillators to select only photons emanating directly from the localized source(s). Laboratory Bench Testing provided physical confirmation that an array of unique, elongated geometry, LaBr₃:Ce sensors performed as predicted by MCNP Modeling to resolve source azimuth direction. The response of each sensor element is anisotropic providing a response dependent on the azimuth of the source relative to the sensor, while the integrated response of the entire array is isotropic, providing a source strength-distance indicator to act as a reference for an original software algorithm that processes each isotope response to determine azimuth. Laboratory tests have confirmed that an array of four (4) sensors would be sufficient to provide $\pm 5^\circ$ azimuth determination over a 360° field of view. The approach accommodates a large volume of scintillation material with minimal shielding <20% compared to about 50% for Coded Aperture approaches to provide a high sensitivity and a wide (360°) field of view. This Patent Pending innovation has been integrated with an iRobot ATRV Robotic Platform and autonomous approach to isotopic sources in a field environment has been demonstrated.

I. INTRODUCTION

The Domestic Nuclear Detection Office (DNDO) of the US Department of Homeland Security (DHS) identified a vital need of Law Enforcement, First Responder and Military Staff responsible for detecting radiological threats. This need is to

advance the state of the art of available omni-directional radiation detection devices, such as Survey Meters and Hand Held Isotope Identification Devices which are sensitive enough to detect many threats, but lack the capability to rapidly determine the type and location of the radiation source from a moderately distant location (10m to 50m). Information from these instruments may be ambiguous and inadequate in both routine inspection and live threat response scenarios given that the main goal is to *find* the radiation source or sources quickly to determine the risk level and the appropriate response. DNDO issued a call for SBIR proposals constraining the required performance to only those parameters that were necessary for operational personnel. Particularly important, these requirements accepted concepts that provided:

- Azimuth in two dimensions only (i.e. three dimensional locations were not mandated).
- Moderately precise, angular resolution of $\pm 10^\circ$ or better.
- Gamma Source Detection only (although Neutron Detection was desired).

The method described herein was demonstrated to meet or exceed these requirement with an angular resolution of $\pm 5^\circ$ and a high sensitivity to gamma sources at a distance of 10m to 50m. The foundation of this technique is that the cumulative response of a total array of sensors with large L/D ratios (e.g. 25mm diameter and 102mm length) in parallel planes and evenly spaced as shown in Fig. 1 would provide an isotropic or azimuth independent cumulative response, while each individual sensor response would be highly anisotropic.

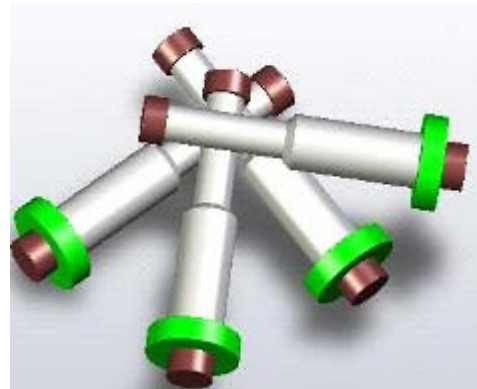


Fig. 1 is a top perspective of the concept arranged as an array of four (4) 25mm X 100mm Scintillators with Photomultiplier Tube Readouts and Trim Shields.

Manuscript received November 16, 2007. This work was supported in part by the US Department of Homeland Security (DHS)-Domestic Nuclear Detection Office (DNDO) Contracts NBCHC060045 and NBCHC070028 and Department of Defense Development Grant: #54144-P3438-B7823.

James H. Winso, Eric S. Ackermann, Michael Fennell, Roger Perez, and John Rolando are with Space Micro Incorporated, San Diego, CA 92121 USA (telephone: 858-332-0700, e-mail: jwinso@spacemicro.com). Manish Pagey was with Space Micro Incorporated during the performance of this work.

Raulf Polichar and Juan Martinez are with Science Applications International Corporation, San Diego, CA 92127 USA (telephone 858-826-9724, e-mail policharr@saic.com).

Jens Hovgaard is with Radiation Solutions Incorporated, Mississauga, Ont, Canada (telephone 905-890-1111, e-mail: hovgaardj@radiationsolutions.ca).

Greg Kogut, Donnie Fellars, H. R. (Bart) Everett, Joel Baumbaugh and Gary Mastny are with the Space and Naval Warfare System Center, San Diego, CA 92106 USA (telephone 619-553-0707, e-mail: greg.kogut@navy.mil).

Preliminary MCNP modeling indicated that each sensor would have a notably different response to a localized source depending upon azimuth, even though the cumulative response of all sensors in the array would not depend on the azimuth of the isotope over a 360° Field of View (FOV). The modeling determined that by exploiting the precise energy resolution of LaBr3:Ce an array would provide the required data for an Angular Determination Algorithm to determine the azimuth of each isotope detected with a relatively high, $\pm 5^\circ$, precision. Each region of interest of the energy spectrum must be analyzed separately since the relative response versus angle is a complex function of energy, thus this process was made practical by considering only those isotopes identified by ANSI 42.34-2003 [1]. This technique is independent of source strength or distance, although weaker or more distant sources will have reduced statistical precision.

The early work, funded by the DNDO Phase I SBIR, was focused on Modeling and Collection of Laboratory Test Bed Data to confirm that the use of Geometrically Optimized Lanthanum Bromide (LaBr3:Ce) Scintillation Crystal Sensors could provide the ($\pm 5^\circ$) Angular Resolution required. Further efforts, described herein, included conducting Field Testing, Constructing a Prototype and demonstrating integration with a Robotic Vehicle.

II. MODELING

The goal of Monte Carlo N-Particle (MCNP) modeling was to continue the work of earlier geometric, single interaction modeling to provide a more accurate and detailed basis for predicting the expected prototype performance as well as refining the planned laboratory test bed experiments. Prior to initiating detailed MCNP modeling the earlier model results were used to select the sensor material and geometry.

A. Sensor Material and Geometry Selection

Since the described approach was based on evaluating the response of each detector for each individual isotope, the isotope identification performance of the scintillation material was vital for the Scintillator. It was clear from many studies (e.g. [2]) that LaBr3 offered superior performance to NaI. Table 1 compiled from data presented in [3] and [4] compares commercially available scintillation material.

TABLE I
COMPARISON OF SCINTILLATOR MATERIAL CANDIDATES

Material	Density (g/cc)	Light Yield (per KeV)	Decay Time (nsec)	Peak λ (nm)	Temp Variation (%/deg C)	FWHM (% at 662KeV)
NaI(Tl)	3.67	38	250	415	0.3%	6.6
CsI(Tl)	4.51	63	900	540	0.2%	6.0
LaCl3:Ce	3.84	45	28	~350	0.1%	4.0
LaBr3:Ce	5.08	63	16	~380	0.04%	<3.0
LYSO	5.4	27	53	445	N/A	10
BGO	7.1	8	300	380	0.8%	10

Table 1 shows that the Saint Gobain Crystals (SGC) BrillanCe 380® LaBr3:Ce Scintillators have a high density (5.08 g/cc) promising a relatively high cross section and high light yield (63 photons per KeV) leading to excellent resolution (<3.0% at 662 KeV) compared to other Scintillators. Although not vital for detection of weak sources, the rapid decay time minimizes concerns about saturation and system paralysis if moved close to intense Radiation Dispersal Devices (RDD) and the Temperature Insensitivity is important for real world devices. Additionally, the Photopeak at 380 nm is well suited for many available Photomultiplier Tubes [5].

B. Modeling Results and Predictions

The MCNP modeling of a 25mm X 102mm LaBr3 Detector with various scenarios of Gamma Radiation Source Strength, Energy and Direction was performed to support the design of the experimental test bed. The sensor configuration modeled is shown in Fig. 2.

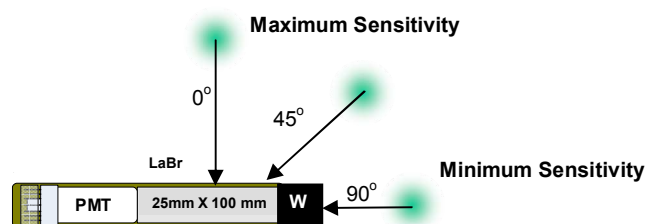


Fig 2 Shows the LaBr3 Scintillator Configuration Modeled.

To account for differing isotope energy the MCNP results from five (5) typical energies of interest for the intended application (180 keV, 330 keV, 660 keV, 1300 keV and 2600 keV) were analyzed to provide a broad spectrum representing the expected operational Fissile, Medical, Industrial and Naturally Occurring Radiation Material sources. The linear absorption coefficient, μ (E), for LaBr3 scintillation crystals was considered as a function of energy to account for these differing isotopic sources. To account for variations in Source Strength, two different count totals (100M and 10M) were used. The distance was arbitrarily set to 1 meter, since it was anticipated that the laboratory experiment would be mostly at 1 meter distance. The impact of a 25mm X 25mm end cap shield, with Lead (Pb) and Tungsten (W) was modeled as well as a pencil beam scenario to estimate the effects of a collimated source. Samples of the plots of the results are shown in Fig. 3 at 330 KeV and Fig. 4 at 1300 KeV. The results of the simulation across the energy band from 180 KeV to 1300 KeV led to the following conclusions and predictions for the experimental test bed:

- Angular Resolution was estimated to be approximately $\pm 5^\circ$ for a source greater than 37 MBq (1 mCi) at 10 Meter distance in less than 1 minute.
- A monotonic response indicating viability of a four (4) sensor array was shown in Fig. 3 for moderate energies although end shields were required to prevent ambiguity for source azimuths near the sensor ends as shown in Figure 4.
- Predicted array sensitivity was identification of 100 MBq (2.7mCi) source @30 meters in << 1minute.

MCNP simulation of LaBr3 (25mm X 100 mm) bombarded with 330keV gamma source at Various Angles with 90 deg side Shielded, Isotropic source with 100M particles

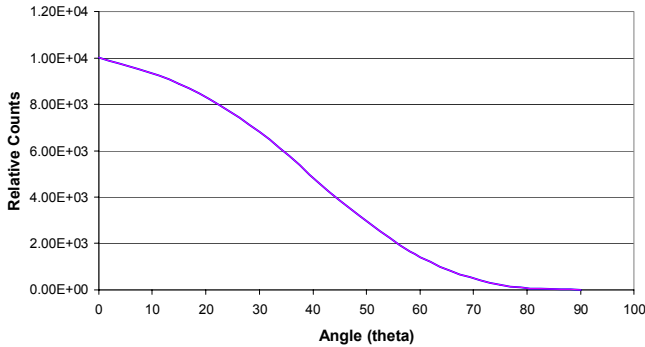


Fig. 3 shows a predictable monotonic response at 330 KeV.

MCNP simulation of LaBr3 (25mm X 100mm) bombarded with 1300keV gamma Isotropic Source with 100M Particles at Various Angles

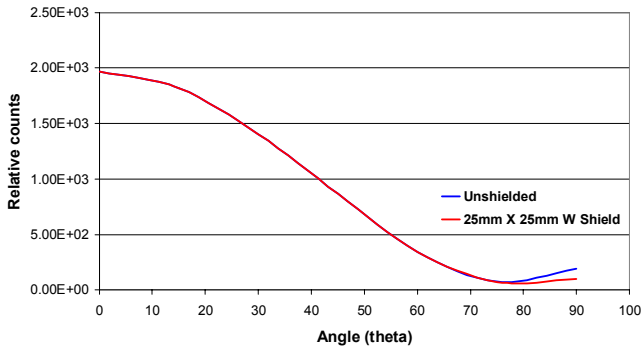


Fig. 4 shows an ambiguous response at 1300 KeV near the sensor axis (blue) indicating the need for End Cap Trim Shields in the Laboratory Test Bed.

III. LABORATORY EXPERIMENTS

To obtain the highest possible energy resolution from the test bed SGC BrillLanCe 380 LaBr3 sensors it was decided the proof of concept should be tested with an L/D ratio of 2:1 for the Scintillators. For this geometry SGC guaranteed an energy resolution of < 3.5% at 662 KeV. The received sensors were tested to verify performance and they demonstrated a resolution of from 2.91% to 3.34% at 662 KeV consistent with SGC factory data. Two 25mm X 51mm LaBr3 sensors were adjoined as illustrated in Fig. 5 to achieve the required 25mm X 100mm geometry modeled.

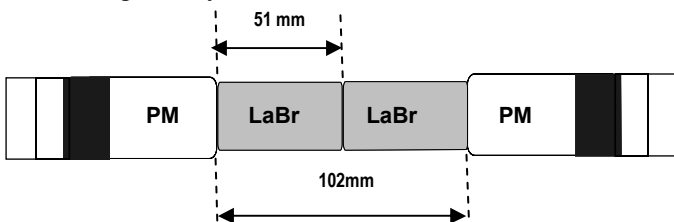


Fig. 5 shows that the 25mm X 100mm LaBr3 configuration modeled by MCNP could be achieved for the test bed by adjoining two 25mm X 51mm sensors.

To confirm the MCNP results it was decided that two sensor arrays as shown in Fig. 5 would be mounted at 90° angles relative to each other (a total of four 25mm X 51mm sensors). The signals from the adjoined sensors would be

added together by the data collection routines and treated as a single detector set. The resultant laboratory test bed is depicted in Fig 6, with source stands, NIM Readouts and the two sensor arrays.

A. Test Bed Data Collection

The sensor mounting plate can be rotated in 5° steps and locked in place with a set pin for accurate angular measurement. The white containers on the ends of the sensors contain powdered tungsten trim shields.



Fig. 6 depicts the four sensors configured as two sensor sets mounted on a swiveling based plate registered at 5° intervals with the source test stand at left.

Over 800 radiation spectra were collected and analyzed with this test bed including multiple angles and multiple source scenarios. The angular resolution was measured with exempt levels of Cs-137, Ba-133, and Co-60, which were spaced at 1 meter and 2 meter distances. Included were responses with both single and multiple sources and with sources elevated out of the horizontal detector plane. The sensors were also tested for angular resolution of the each of the isotopic sources in a high intensity background created by attaching a set of Coleman Lantern Mantles directly to the Sensors. Additionally overnight data collection to measure sensitivity to the 2.6 MeV thorium peaks validating the high energy performance of the sensors and tests were conducted to observe the variation in the channel of the La-138 peak relative to other photo peaks at temperature extremes.

B. Laboratory Test Bed Results

The result of the difference in the response of sensors dependent upon angle is shown in Fig. 7.

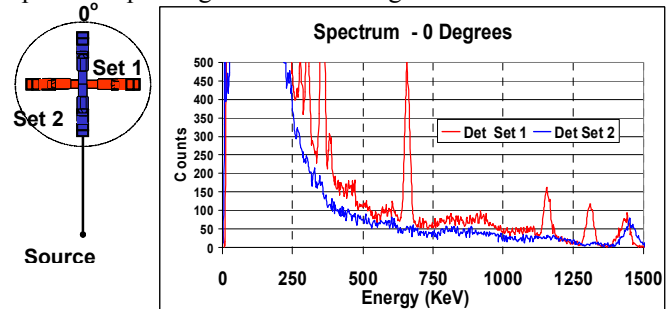


Fig. 7 includes the spectra from both Laboratory Detector Sets when exposed to simultaneous sources. The four peaks at the left are the Ba-133 peaks including the 383 KeV peak. The center peak is Cs-137 and the two peaks to

the right are Co-60. The far right peak is the La-138 Peak. Each channel is 2.75 KeV.

Contrasting the data of Fig. 7, which was arbitrarily referenced as 0° with Detector Set 2 (Blue) pointing directly at the source is Fig. 8, which shows the response when rotated 90° to reference position 90° so that Detector Set 1 (Red) is pointing directly at the source.

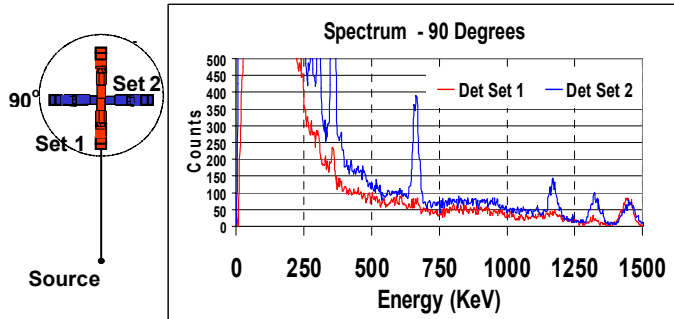


Fig. 8 includes the spectra from both Laboratory Detector Sets when the array consisting of both detector sets is rotated 90 degrees. Each channel is 2.75 KeV.

By calculating the ratio for each isotope as the array is rotated in 5° steps a curve of the relative intensities versus angle is recorded for each isotope. Fig. 9 shows the spectrum from 30° as an example of an intermediate angle. Note that the ratio of the detector set is dependent on the isotope. In particular, Fig. 9 shows that the ratio for the Cs-137 662KeV peak is greater than for the 1.17 MeV and 1.3 MeV peaks of Co-60. This is because the 25mm thickness of the LaBr3 cylinder is more transparent to the higher energy, providing a more shallow angular response curve. Even the high energy Co-60 showed a consistent variation of 1% per degree or more was observed over a 45° range of response.

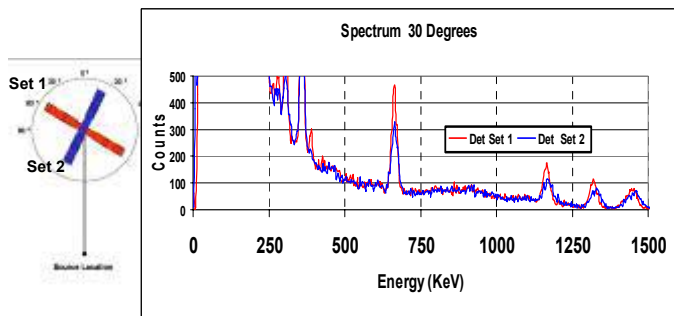


Fig. 9 includes the spectra from both Laboratory Detector Sets when the array consisting of both detector sets is rotated 30 degrees. Each channel is 2.75 KeV.

The ratios of the relative sensor response was collected for each angle and plotted for each isotope. An example for a 300 KBq (8.1 μCi) Cs-137, source at 2 meters is shown in Fig. 10. It shows the greatest variability is for the detector pointed most closely towards the source. Since this was only a two detector array, an ambiguity did exist, which could be resolved by rotating the array. This data was then projected for a four sensor array and showed that the cumulative results of the array would be isotropic while the individual sensors would be very anisotropic providing the algorithm with the ability to calculate the azimuth for each isotope. Informal blind testing

administered by DNDO demonstrated an angular resolution determination within ±5° in the laboratory.

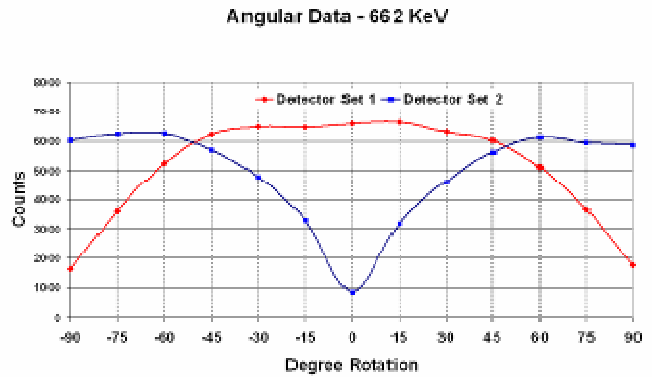


Fig. 10 shows the variation of response is greatest near the 0° position (Detector Set 2 pointing towards the source) providing sufficient raw data for the Azimuth Determination Algorithm to calculate the source angle.

The response characteristics have some similarities to the rotating modulation collimator [6], however even though the information is a ray with two vectors 180° apart that could be resolved with source motion, motion of collimation shielding is not required. Perhaps, even more important, by using very small amount of end cap shielding, the RadSITE™ approach allows over 80% of the source photons to reach the sensor array, providing a high sensitivity for detection and identification as well as azimuth determination.

The laboratory results demonstrated that Multiple Sources could be detected simultaneously, that sources could be located at variable distances and that sources elevated out of the horizontal detector plane could be located with some limitations. If multiple sources of the same isotope are present at different vectors the system will locate the source with the highest intensity to distance squared ratio, provided the ratio is a factor of two higher. If this ratio is near unity resolution of the location would require motion of the sensor.

IV. FIELD DATA

The laboratory effort described in the previous section led to specifying two 25mm X 102 mm BrillLanCe 380® Detectors from SGC for collection of field data and construction of a field prototype. Upon receipt the detectors were tested to verify performance and they demonstrated a resolution of 3.34% to 3.50% at 662 KeV meeting the specification. Intrinsic Lanthanum (La-138) background data was also collected over 15 minute intervals in a lead (Pb) cave, which confirmed that the intrinsic source produced approximately 1.2 cps per cc as published by Saint Gobain Crystals [7].

Shielded La-138 Background

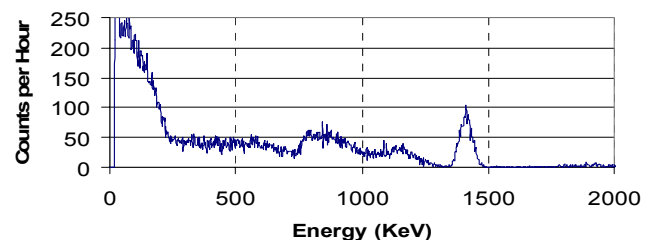


Fig. 11 shows the 15 minute data collected from shielded 25mm X 102mm BrillLanCe 380 Sensors to measure the La-138 background. It indicates 1.21

cps/cc (.05 cps/cc in 1.41 MeV Region of Interest). Each channel is 2.75 KeV.

The detector data was read out through a Canberra uniSpec® collection system to a PC and they were placed on a cart to facilitate collection of data at Battery Woodward, a WWII bunker located at the US Navy Space and Naval Warfare System Center (SSC-San Diego) San Diego, CA facility. An overhead plan view of Battery Woodward is shown in Fig. 12. To provide perspective, it is noted that the distance from position S1 on Fig. 12 to the Ba-133 Source at left is approximately 30 meters. This facility capably simulated an underground urban environment.

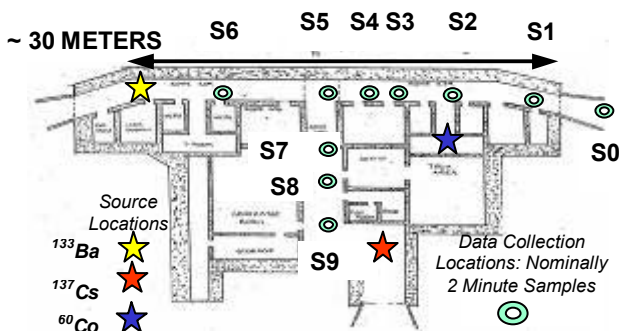


Fig. 12 is a plan view of Battery Woodward with Ba-133, Cs-137 and Co-60 deployed to simulate an urban environment with intense source interference.

Three sealed sources were simultaneously deployed in the bunker at the locations indicated by stars. They included a 74 MBq (2 mCi) Ba-133 source, a 518 MBq (14 mCi) Co-60 source, and a 2 GBq (54 mCi) Cs-137 source. The purpose of the data collection was to characterize sensor performance with multiple sources. In particular, it was important to determine if a smaller Ba-133 source could be located in an interference caused by two larger sources, the Co-60 a few meters from the main corridor and the very large Cs-137 located in a scatter rich location. One or more two minute samples were taken at 10 locations in Battery Woodward as shown by the donut rings labeled S0 through S9 on Fig. 12. Background readings were collected at location S0 both prior to and after deploying the sources.

The spectrum in Fig. 13 shows that the 74 MBq (2 mCi) Ba-133 source was detected, located and the azimuth determined in ~2 minutes at location S1 at a distance of 30 Meters. It was also located at locations S3, S4 S5, and S6 (Fig 14, with source stand visible). The Ba-133 was not observable at location S2 due to Co-60 source interference.

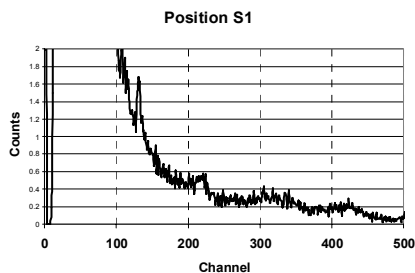


Fig. 13 shows the Field Data Collection Apparatus at Position S1 looking down the main corridor approximately 30 meters toward the Ba-133 Source.

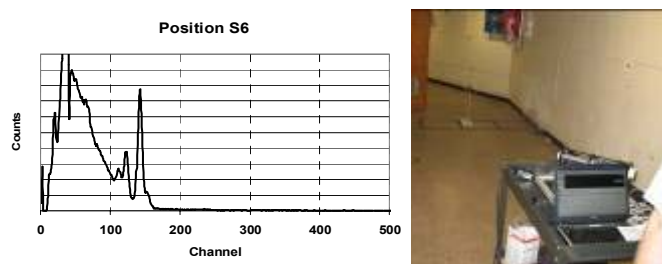


Fig. 14 shows the Field Data Collection Apparatus at Position S6 with the Source Stand holding the Ba-133 Isotope approximately 6 meters distant.

At location S7 the Cs-137 source was easily detected, but not identified or located, while at S8 it was identified and at S9 it was located. Closer approaches to less than a meter from the Cs-137 source provided valuable saturation data.

V. PROTOTYPE INSTRUMENT

The two (25mm X 102mm) BriLanCe 380® LaBr3 Detectors were integrated into a self contained field prototype to demonstrate operation as shown in Fig. 15. The enclosure included a COTS Preamp, Shaper and MCA, a Single Board Computer and both High and Low Voltage Power Supplies. The unit also included a rechargeable battery pack, sufficient for over 4.5 hours of stand alone operation and was also able to be powered by 120VAC. Data interfaces were through Dual Ethernet connections to allow for diagnostics to be performed in parallel with data collection.

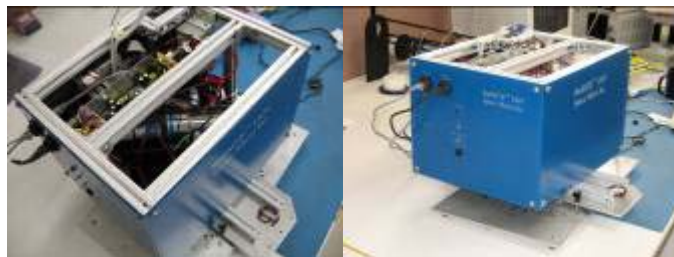


Fig. 15 shows a top view and side view of the Field Prototype Unit.

The Field Prototype Unit was intended as a Test Bed to demonstrate the capability of the technology to withstand moderate field environments, thus there were minimal size and weight constraints. The prototype weighs about 14 KG and the enclosure dimensions are 40cm X 33cm X 25cm. It is believed that the next prototype, currently in work, will substantially reduce the footprint and mass, since the next generation of sensors has been reduced in size and tailored circuitry is replacing many of the COTS packages.

An Interface Control Document (ICD) was developed to enable integration with a readout system or robotic platform. The data provided includes total counts, source strength for identified isotopic sources (normalized for 10 meter distance), azimuth for identified isotopes with confidence factors and diagnostic data. Data is provided in response to requests only and is contained in four time buffers of 10, 20, 50 and 120 seconds. For diagnostic purposes data is stored internally at every 10 second interval and is available for 300 seconds in a FIFO buffer.

VI. ROBOTIC INTEGRATION

The Field Prototype was integrated with a US Navy SSC-San Diego, Unmanned System Branch iRobot ATRV Platform to demonstrate autonomous source detection, identification and location. The RadSITE™ unit provided data to the ATRV through an Ethernet connection (the only connection between the RadSITE™ and the ATRV) as described in Section V. The ATRV is an older platform, but was chosen because the payload capability was compatible with the prototype's dimensions and weight. The ATRV also runs on rechargeable batteries and is capable of operating for 4 hours without recharging. Fig. 16 shows the Field Prototype being integrated with the ATRV Platform.



Fig. 16 shows the Field Prototype mounted to the ATRV Unmanned Ground Vehicle. Each unit contains its own rechargeable battery pack.

A. System Characteristics

Although an older platform the Software Package on the ATRV is compatible with the Software Package on the ATRV is compatible with currently fielded small Unmanned Ground Vehicles, including the iRobot Packbot and Foster-Miller Talon. The ATRV Instrument Package includes LIDAR for obstacle avoidance, GPS for Positional Awareness and Electronic Compass for Azimuth Information. It is compatible with camera systems and maintains wireless communications with its base station. It is capable of autonomous tracking missions and thus very well suited for the Autonomous Gamma Source Direction Finder Mission or for Orphan Source Detection as defined in [8]. The software is quite mature, but still evolving. US Navy SSC-San Diego Unmanned Systems Branch scientific and technical staff developed all of the tracking routines specific to Gamma Source Tracking with input from the Space Micro Gamma Source Locator as defined by the agreed upon ICD.

B. Autonomous Source Detection

As noted above the RadSITE™ Prototype provides data to the ATRV Platform in several Time Buffers, but experience indicated that the system was sensitive enough to use the 20 second Time Buffer exclusively, thus simplifying the interface. To initiate a search the ATRV was instructed to enter a search zone using a standard search algorithm developed by SSC-San Diego Technical Staff. When a source is detected by gross counts or by counts within a specified Convolved Region of Interest, the ATRV will halt and collect azimuth data, nominally for a 1 minute interval depending upon the angular confidence factor. Since the

prototype only has two detectors two potential angles are identified, but assuming the source is ahead it is generally in the same quadrant (an exception is 0° or straight ahead, which might also be either left or right). The robot will then turn in the direction of the source or in an arbitrary direction if the source is potentially at 0° and collect another sample to disambiguate the vectors. When the correct vector is chosen, the robot will move 2 meters in that direction assuming no obstacles, stop and take another sample. Using this information the ATRV confirms that the source is indeed forward and using simple $1/r^2$ will calculate the approximate strength and distance values. The vehicle then moves $\frac{1}{2}$ the distance to the source and repeat the process until within an arbitrarily defined distance (e.g. 1 meter) from the source. Fig. 17 shows the ATRV taking a sample and then moving to the target source, which is on the seat of the vehicle in the photo. This was a 17.4 MBq (470 μ Ci) Cs-137 source, which was detected and tracked from a distance of 17 meters.



Fig. 17 shows the US Navy Unmanned Systems Branch ATRV autonomously tracking a source to its location in a pickup truck. This track was made easy by the absence of obstacles between the ATRV and the source.

The SSC-San Diego Robots are capable of much more effective tracking algorithms to include triangulation and obstacle avoidance routines, which are included in the standard SSC-San Diego Robotic packages. Work on integrating these with RadSITE™ is progressing as shown in Fig. 18, which also shows a camera which automatically points to the source during the sampling period. Transmission of this visual information to the operator during the sampling and tracking process is a significant tool for facilitating threat assessment.



Fig. 18 shows the ATRV camera pointing to the source prior to tracking.

Additional efforts are under way to reduce the unit's size, incorporate more sophisticated spectral deconvolution algorithms to facilitate airborne operations as noted in [9], expand the library of isotopes, improve the response time and to track moving sources.

VII. CONCLUSIONS

An advantage to the method discussed is that it will *detect and identify* sources over a 360° Field of View and since it does not use Coded Aperture or Collimation Shielding which absorb approximately 50% of the incoming photons; it is inherently more sensitive than those approaches. Laboratory and field testing has demonstrated moderate stand-off detection and identification of localized gamma sources within about 20 seconds for 37 MBq (1 mCi) to 370 MBq (10 mCi) level isotopes at 10m to 30m distance.

The *angular resolution* observed in the laboratory and the field has provided a confident determination of azimuth within about 1 minute to a precision of $\pm 5^\circ$ for sources at the strength and distance listed above. This ability has been demonstrated for simultaneous azimuth vector determination of multiple Isotopic Sources. This ability has also been demonstrated in the presence of intense background, although dispersed sources of the same isotope at approximately the same flux level (intensity-distance squared ratio) will result in ambiguous vectors; however rotation of the array will indicate the presence of multiple sources. The azimuth of sources raised or lowered out of the horizontal detection plane will be measured with some limitations for large angles (e.g. $> 30^\circ$) dependent upon the relative arrangement of sensors.

An additional important aspect for application of this technology is the cost outlook. Since the driving factor for cost is the LaBr3 Sensor, it is encouraging that the comparable cost for a given volume of Saint Gobain Crystals BrillanCe® 380 has dropped nearly 50% over the last 2 years while performance has continually improved. The Field Demonstration of the ability to guide a SSC-San Diego, Unmanned Systems Branch autonomous vehicle to a source without operator intervention has shown the potential power of applying this method as an effective tool for responding to or searching for potential radiological threats.

ACKNOWLEDGMENT

This work was supported in part by the US Department of Homeland Security (DHS)-Domestic Nuclear Detection Office (DNDO) Contracts NBCHC060045 and NBCHC070028 and Department of Defense Development Grant: #54144-P3438-B7823. We also acknowledge the valuable loan of precision laboratory equipment by SAIC that facilitated the initial data collection. We also received valuable collaboration from Saint Gobain Crystals, to modify the BrillanCe 380 performance for the direction finding application. The exceptional technical support the operational counseling received from the US Navy Unmanned System Branch for integration of the Space Micro Inc. technology on the Standard US Navy Robotic Platform has been unparalleled. Additionally, the SSC-San Diego Radiation Safety Office assistance to make the required sources available and to ensure that they were properly deployed was vital to the progress made to date.

REFERENCES

- [1] American National Standard Performance Criteria for Hand-held Instruments for the Detection and Identification of Radionuclides, ANSI 42.34-2003, page 11.
- [2] B. D. Milbrath, B. J. Choate, J. E. Fast, W. K. Hensley, R. T. Kouzes, J. E. Schweppe, "Comparison of LaBr3 and NaI(Tl) Scintillators for Radioactive Isotope Identification Devices", Pacific Northwest National Laboratory, Richland, WA, USA
- [3] C. M. Rozsa, M. R. Mayhugh, P. R. Menge, "Two new Scintillators: LaCl3: Ce and LaBr3: Ce", SPIE, Aug 14, 2006.
- [4] Peter R. Menge, Alain Iltis, Guillaume Gautier, Vladimar Soloyvez, "Performance of Large Lanthanum Bromide Scintillators", Symposium on Radiation Measurements and Application (SORMA), May 23-26, 2006
- [5] R. Mirzoyan, M. Laatiaouia, M. Teshimaa, "Very high quantum efficiency PMTs with bialkali photo-cathode", Nuclear Instruments and Methods in Physics Research Section A: Accelerators, Spectrometers, Detectors and Associated Equipment, Volume 567, Issue 1, 1 November 2006, Pages 230-232
- [6] D. M. Smith, G. J. Hurford and S. E. Boggs, "Rotating modulation collimator imagers", *New Astronomy Reviews, Volume 48, Issues 1-4, February 2004, Pages 209-213*
- [7] C. Dathy, P. V. Ouspenski, Recent Results with Large Volume LaBr3 and LaCl3 Scintillator Detectors, IEEE NSS (2006), St Gobain Crystals, Nemours, France
- [8] R. R. Finck, T. Ulvsand, "Search for Orphan Gamma Radiation Sources: Experiences from the Barents Rescue 2001 Exercise", Proceedings of the International Atomic Energy Agency conference on Security of Radioactive Sources, March 10-13, 2003, Vienna Austria, pp 123 to 138.
- [9] Hovgaard J., "Airborne gamma-ray spectrometry : Statistical analysis of airborne gamma-ray spectra", PhD thesis, Technical University of Denmark ID: Hovgaard, J
- [10] Radiation Detection and Measurement, Glenn F. Knoll, John Wiley and Sons, 1979, pp 238 to 353.